

Artigo Original

Recebido em 22/11/2001 e aceito em 12/04/2002

**A coherence-based technique
for evaluating the degree of
synchronism in the EEG during
sensory stimulation**

Técnica baseada na função de coerência para avaliar o grau de sincronismo no EEG durante estimulação sensorial

Antonio Mauricio F.L. Miranda de Sá

Departamento de Eletricidade (DEPEL)
Fundação de Ensino Superior
de São João del Rei – FUNREI
Praça Frei Orlando, 170, Centro
São João del Rei, MG, Brazil - CEP: 36307-352
Tel: 55 - 032 3379-2553, Fax: 55 - 032 3379-2360
e-mail: amiranda@funrei.br

Antonio Fernando Catelli Infantosi

Professor Titular
Programa de Engenharia Biomédica - COPPE/UFRJ
e-mail: afci@peb.ufrj.br

Abstract

The coherence between the stimulation signal and the EEG has been used in the detection of evoked responses to rhythmic stimulation. Such detection is based on the knowledge of the sampling distribution of coherence estimate under the null hypothesis of lack of evoked response (zero coherence). In this work, the technique is extended for quantifying the degree of activation due to sensory stimulation. With this aim the sampling distribution for the non-zero response is investigated for evaluating the performance of the detector as well as obtaining the confidence limits of coherence estimate. The latter are obtained using an approximation to the probability density function of the estimate, since the closed-form inverse for the cumulative density function, and hence the critical values for non-zero coherence, cannot easily be found. The theoretical results are verified in Monte Carlo simulations and the technique is further applied to the EEG signals from 14 subjects during rhythmic photic stimulation. The results indicate inter-hemispheric symmetry at homologue posterior regions in the stimulation frequency of 6 Hz and also its harmonics for most of the subjects. As expected, such symmetry is more pronounced at occipital regions. Further, in 28% of the subjects, the strength of the responses in 12 Hz depends on either such frequency is the stimulation frequency or the second harmonic of it. This difference may be due the fact that the stimulation frequency is lower or higher the subjects' alpha rhythm and need to be further investigated. **Keywords:** Coherence, EEG, Rhythmic, Statistics, Stimulation, Synchrony Measure

Resumo

A coerência entre o sinal de estimulação e o EEG tem sido utilizada na detecção de respostas evocadas à estimulação rítmica. Tal detecção baseia-se no conhecimento da distribuição amostral da estimativa da coerência sob a hipótese nula de ausência de resposta evocada (coerência igual a zero). Neste trabalho, a técnica é estendida para a quantificação do grau de ativação devido à estimulação sensorial. Para isto, a distribuição amostral para o caso de resposta diferente de zero é investigada, objetivando avaliar o desempenho do detector assim como os limites de confiança das estimativas da coerência. Estes últimos são obtidos através de uma aproximação à função densidade de probabilidade da estimativa, pois a inversa da função densidade acumulada de probabilidade não é de fácil obtenção, o que dificulta a determinação dos valores críticos para coerência diferente de zero. Os resultados teóricos são verificados em simulações de Monte Carlo e a técnica proposta é aplicada a sinais EEG de 14 indivíduos durante foto-estimulação rítmica. Os resultados mostram simetria inter-hemisférica em regiões posteriores homólogas na frequência de estimulação de 6 Hz e seus harmônicos para a maioria dos indivíduos. Tal simetria, como esperado, é mais pronunciada nas regiões occipitais. Ademais, em 28% dos indivíduos, a intensidade das respostas em 12 Hz depende se esta frequência é a de estimulação ou o segundo harmônico da mesma. Esta diferença parece depender da frequência de estimulação ser inferior ou superior ao ritmo alfa do indivíduo. **Palavras Chave:** Coerência, EEG, Estatística, Estimulação Rítmica, Medida de Sincronismo.

Introduction

The coherence function has been extensively used as a tool for quantifying the similarity between signals in the electroencephalogram (EEG). While the correlation coefficient provides a global measure in such quantification, coherence is selective in frequency, with the additional benefit that its magnitude is independent of any time delay between the signals. Evoked responses to sensory stimulation are used in the clinical practice, as a neurophysiological exam in which a fixed, periodic stimulus is applied to the human sensory system, eliciting a response in the electrical brain activity picked up in the EEG from the scalp above the relevant cerebral area. Since these responses are small, averaging techniques over many stimuli are used for revealing the cerebral response.

Techniques have been developed with the aim of statistically testing for the presence of such responses. They allow, for instance, accessing the integrity of neuronal paths during surgeries involving the spinal cord or evaluating auditory deficits in new-borns (Chiappa, 1997). The coherence between the stimulation signal and the EEG can be taken as an example of such techniques. It has been reported as a powerful tool in the detection of evoked responses (Dobie and Wilson, 1996). A reason for this is the fact that the detector is very robust, since the threshold is independent of both the shape of the response and the signal-to-noise ratio (SNR) (Carter, 1993). Thus, the detection of responses is achieved by comparing the estimated coherence with a threshold, which is obtained based on its well known sampling distribution under the null hypothesis of zero coherence (absence of evoked responses). Additionally, coherence can be estimated in this case using only the EEG signal, leading to a simpler expression to be computed, as well as reducing random errors due to noise in data acquisition. The technique was proposed by Dobie and Wilson (1989) for detecting auditory evoked potentials, and has been used by these authors in the same field (Dobie and Wilson, 1996) and by others in somatosensory (Tierra-Criollo *et al.*, 2000) and visual potentials (Miranda de Sá *et al.*, 2001).

However, in order to evaluate the detector's performance, the probability of detecting a response if such is present must be obtained. It will be carried out based on the sampling distribution for the non-zero response case (Miranda de Sá, 2000) and using an approximation which permits the confidence limits for coherence estimates to be determined. By doing in this way, the technique is extended for quantifying

the degree of activation due to sensory stimulation. The results are verified by Monte Carlo simulations and further tested on EEG signals from 14 subjects during rhythmic photic stimulation.

Coherence between a random and a periodic

signal - $\hat{\kappa}_y^2(f)$

The coherence estimate between two random, finite length record, discrete-time signals, $x[k]$ and $y[k]$ may be obtained using the well known approach of dividing the signals into M segments as (Bendat and Piersol, 2000):

$$\hat{\gamma}_{xy}^2(f) = \frac{\left| \sum_{i=1}^M X_i^*(f) Y_i(f) \right|^2}{\sum_{i=1}^M |X_i(f)|^2 \cdot \sum_{i=1}^M |Y_i(f)|^2} \quad (1)$$

where “^” and “*” (superscript) denote, respectively, estimation and complex conjugate, $X_i(f)$ and $Y_i(f)$ are the T -length Fourier transforms of the i th windowed data segments and M is the number of segments used in the estimation. For the particular case when $x[k]$ is a deterministic, periodic signal (as in the case of periodic stimulation), $X_i(f)$ is identical in each data-window, say $X(f)$, leading to the following simplification:

$$\begin{aligned} \hat{\gamma}_{xy}^2(f) \Big|_{x[k] \text{ periodic}} &= \frac{\left| \sum_{i=1}^M X^*(f) Y_i(f) \right|^2}{\sum_{i=1}^M |X(f)|^2 \cdot \sum_{i=1}^M |Y_i(f)|^2} \\ &= \frac{|X(f)|^2 \left| \sum_{i=1}^M Y_i(f) \right|^2}{M |X(f)|^2 \cdot \sum_{i=1}^M |Y_i(f)|^2} = \frac{\left| \sum_{i=1}^M Y_i(f) \right|^2}{M \sum_{i=1}^M |Y_i(f)|^2} \quad (2) \end{aligned}$$

In order to distinguish from the generic $\hat{\gamma}_{xy}^2(f)$, the coherence between one random and one periodic signal will be denoted in this work as $\hat{\kappa}_y^2(f)$. Thus:

$$\hat{\kappa}_y^2(f) = \frac{\left| \sum_{i=1}^M Y_i(f) \right|^2}{M \sum_{i=1}^M |Y_i(f)|^2} \quad (3)$$

The true value of $\hat{\kappa}_y^2(f)$ for a given window length $(T) - \hat{\kappa}_y^2(f) -$ is obtained by letting $M \rightarrow \infty$ in (3) as:

$$\kappa_y^2(f) = \frac{|E[Y(f)]|^2}{E[|Y(f)|^2]} \quad (4)$$

The estimate $\hat{\kappa}_y^2(f)$ should not, strictly, be considered an estimate of coherence when both signals contain the same periodic activity, as at the frequency of oscillation coherence always assumes a value of one and its use is therefore inappropriate. It can however readily be shown [see expression (8)] that $\hat{\kappa}_y^2(f)$ is related to the signal-to-noise ratio of the response in the frequency bin centred on f (and width defined by the window-length T) and thus provides a useful tool in quantifying the strength of stimulus-responses.

Sampling distribution of $\hat{\kappa}_y^2(f)$

The sampling distribution $\hat{\kappa}_y^2(f)$ is now derived based on the model of Figure 1. Assuming $x[k]$ to be a periodic, deterministic signal, it can be shown (see Appendix 1) that:

$$(M-1) \frac{\hat{\kappa}_y^2(f)}{1 - \hat{\kappa}_y^2(f)} \sim F'_{2,2(M-1)}(\lambda) \quad (5)$$

where $F'_{2,2(M-1)}(\lambda)$ is the non-central F-distribution (Kay, 1998) with 2 and $2(M-1)$ degrees of freedom, and non-centrality parameter λ given as:

$$\lambda = \frac{M |H(f)|^2 |X(f)|^2}{\sigma_f^2} = 2M \frac{\kappa_y^2(f)}{1 - \kappa_y^2(f)} \quad (6)$$

where σ_f^2 is the variance of both real and imaginary parts of $N(f)$. The last equality in (6) may be explained by substituting $Y(f) = H(f)X(f) + N(f)$ in (4). Thus, since $H(f)X(f)$ and $N(f)$ are uncorrelated, it follows that:

$$\begin{aligned} \kappa_y^2(f) &= \frac{|E[H(f)X(f) + N(f)]|^2}{E[|H(f)X(f) + N(f)|^2]} \\ &= \frac{|H(f)|^2 |X(f)|^2}{|H(f)|^2 |X(f)|^2 + 2\sigma_f^2} \end{aligned} \quad (7)$$

and hence

$$\frac{|H(f)|^2 |X(f)|^2}{2\sigma_f^2} = \frac{\kappa_y^2(f)}{1 - \kappa_y^2(f)} = SNR \quad (8)$$

where SNR is the signal-to-noise ratio, which is given in dB as:

$$(SNR)_{dB} = 10 \log(SNR) = 10 \log\left(\frac{\kappa_y^2(f)}{1 - \kappa_y^2(f)}\right) \quad (9)$$

Expression (5) corresponds to the hypothesis H_1 of presence of responses. The null hypothesis (zero coherence) may be obtained as a special case by setting $\kappa_y^2(f) = 0$ in (6) and hence $\lambda = 0$ in (5). Such assumption leads the right hand side of (5) to become the well know (central) F distribution with 2 and $2(M-1)$ degrees of freedom, which is the same distribution as that for the coherence between two Gaussian, uncorrelated signals (Koopmans, 1974). This is explained since the statistics of coherence estimates are invariant with respect to the distribution of one signal, provided the other is Gaussian (Nuttall, 1981). Critical values for $\hat{\kappa}_y^2(f)$, which are the threshold for the detection of evoked responses, are thus obtained as a special case of (5) when $\lambda = 0$ as:

$$\hat{\kappa}_{crit}^2 = \frac{F_{crit,\alpha,2,2(M-1)}}{M-1 + F_{crit,\alpha,2,2(M-1)}} \quad (10)$$

where $F_{crit,\alpha,2,2(M-1)}$ is the critical value of the F-distribution for a significance level α . Thus, for $\hat{\kappa}_y^2(f) < \hat{\kappa}_{crit}^2$, the absence of an additive periodic component can be accepted.

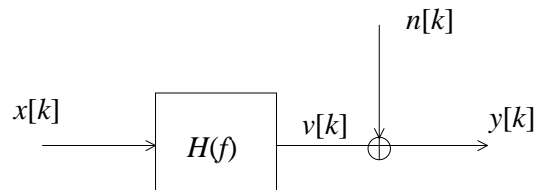


Figure 1. Model for the EEG with an additive stimulus response. $x[k] \leftrightarrow X(f)$ is the stimulating pulse-train, $v[k] \leftrightarrow V(f)$ the response, $n[k] \leftrightarrow N(f)$ is the uncorrelated background EEG, $y[k] \leftrightarrow Y(f)$ the measured EEG and $H(f)$ is the transfer function.

Probability of detection

From (5), the probability of detecting (PD) a response embedded in noise can be determined. This corresponds to the power of the test, or the complement of the false negative rate, β . PD is obtained by evaluating the integral of the non-central F probability density function (PDF) in expression (5) for abscise values greater than $Fcrit_{\alpha,2,2(M-1)}$ defined in (10). This process is illustrated in Figure 2 and is not a trivial task, since it generally requires numerical techniques as pointed out by Kay (1998, p. 30). Fortunately, there is a simple expression (Johnson et al., 1995, p. 485) for evaluating the cumulative density function (CDF) in the special case when the degree of freedom in the denominator is an even integer, as is the case here: $v_2 = 2(M-1)$. Thus:

$$PD = 1 - e^{-\frac{M \kappa_y^2(f)}{1 - \kappa_y^2(f)} (1 - Y')} \times \sum_{i=0}^{M-2} \frac{\left[\frac{M \kappa_y^2(f)}{1 - \kappa_y^2(f)} (1 - Y') \right]^i}{i!} \cdot I_Y(1+i, M-1-i) \tag{11}$$

where $Y' = 2Fcrit_{\alpha,2,2(M-1)} / [2Fcrit_{\alpha,2,2(M-1)} + 2(M-1)]$ and $I_Y(p,q)$ is the incomplete beta function ratio (Johnson et al., 1995, p. 211).

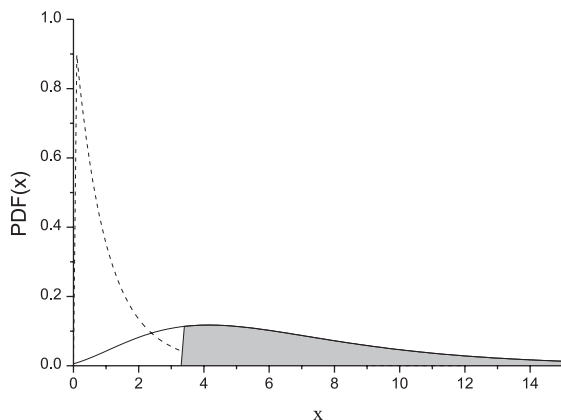


Figure 2. Illustration of the PD calculation as the shaded area under the probability density function (PDF) of the non-central F-distribution defined in (5) (continuous line). The inferior limit is given as the critical value of the distribution under the null-hypothesis, whose PDF is plotted in dashed line.

Confidence limits for $\hat{\kappa}_y^2(f)$

Confidence limits are more readily obtained by using approximations to the non-central F distribution. Patnaik (1949), proposed an approximation fitting a central to the non-central F distribution such that the first two moments are preserved. Applying this to (5), approximate critical values for $\hat{\kappa}_y^2(f)$ may be estimated as:

$$\hat{\kappa}_{crit}^2(f) = \frac{\left[1 + M \frac{\kappa_y^2(f)}{1 - \kappa_y^2(f)} \right] Fcrit_{\alpha, v', 2(M-1)}}{M - 1 + \left[1 + M \frac{\kappa_y^2(f)}{1 - \kappa_y^2(f)} \right] Fcrit_{\alpha, v', 2(M-1)}} \tag{12}$$

where $v' = \left(2 + 2M \frac{\kappa_y^2(f)}{1 - \kappa_y^2(f)} \right)^2 / \left(2 + 4M \frac{\kappa_y^2(f)}{1 - \kappa_y^2(f)} \right)$

Simulation studies

Considering the model of Figure 1, signals $y[k]$ can be generated related to a given $\kappa_y^2(f)$ as (Miranda de Sá, 2000, p. 77):

$$y[k] = \frac{f_s}{f_e} \sqrt{\frac{\sigma_n^2 \kappa_y^2(f)}{L[1 - \kappa_y^2(f)]}} x[k] + n[k] \tag{13}$$

where f_s is sampling frequency, f_e is the frequency of the unit impulse train $x[k]$, L is the number of points used in each window for Fourier Transform calculation and σ_n^2 is the variance of the noise term $n[k]$.

Alternatively, the equivalent to (13) may be carried out in the frequency domain by adjusting the power of the evoked response $v[k] = |H(f)|^2 |X(f)|^2$ - in the model of Figure 1 using the relationship in (8). Thus the values of the i^{th} -window Fourier Transform of $y[k]$ in the frequency (and harmonics) of $x[k]$ may be obtained as :

$$Y_i(f) = \left(\sqrt{\frac{2\sigma_f^2 \cdot \kappa_y^2(f)}{1 - \kappa_y^2(f)}} + N_{Ri} \right) + jN_{Ii} \tag{14}$$

where N_{Ri} and N_{Ii} are, respectively, the real and imaginary parts of the i^{th} -window of $N(f)$, which are zero mean, normally distributed, random variables with variance $\sigma_f^2 = \frac{L}{2} \sigma_n^2$ (Miranda de Sá, 2000, p. 140-141).

Probability of detection

Values of $Y_i(f)$ were generated using (14) with $\kappa_y^2(f)$ ranging from 0.01 to 0.99 in steps of 0.01. The complex noise signal $N(f)$ was generated from unit

variance ($\sigma_f^2 = 1$), normally distributed random numbers for both the real and the imaginary parts. $\hat{\kappa}_y^2(f)$ was then estimated using (3), for $M = 6, 12, 24$ and 48 , and PD-values were obtained by counting the cases in which $\hat{\kappa}_y^2(f)$ was larger than the critical values computed according to (10). The results are shown in Figure 3a (dashed lines) for 1000 $\hat{\kappa}_y^2(f)$ estimates together with those obtained from the theory (solid lines). Note that the experimental values varies around the theoretical ones due to random errors, which become much lower as the number of estimates increase, as can be seen in Figure 2b for 10000 $\hat{\kappa}_y^2(f)$ estimates.

Confidence Limits

Figure 4 shows the confidence limits for $\hat{\kappa}_y^2(f)$ as a function of true $\kappa_y^2(f)$, and for a range of M , calculated according to (12) with the approximation of Patnaik (1949). These were also tested by Monte Carlo simulation ($Y(f)$ generated using (14), but with $\hat{\kappa}_y^2(f)$ ranging from 0 to 1 in steps of 0.1 and using $N = 10000$ iterations, which have been proved to lead to reduced random errors), particularly in view of the

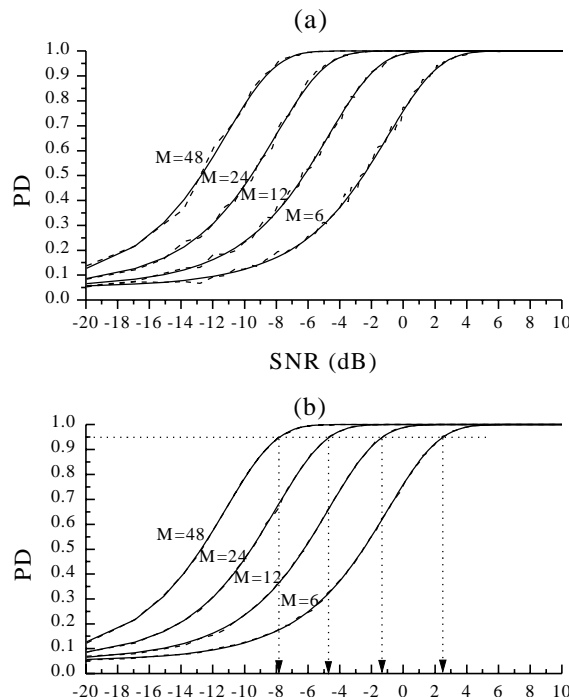


Figure 3. PD-values ($\alpha = 0.05$) as a function of SNR for $M = 6, 12, 24$ and 48 . Experimental (dashed lines) and theoretical values (solid lines) for $N = 1000$ iterations (a) and $N = 10000$ iterations (b). SNR-values for which PD = 0.95 are indicated by arrows.

approximations employed. From these values, experimental inferior and superior limits were found as the 2.5th and 97.5th percentiles, for $M = 6, 12, 24$ and 48 and are shown in Figure 3 as dashed lines. Good agreement with the theoretical values can generally be observed, especially for $M \geq 12$. However, for small values of M and $\kappa_y^2(f) < 0.5$, $\hat{\kappa}_y^2(f)$ extends to lower values than predicted from the theory.

Evaluation of $\hat{\kappa}_y^2(f)$ with simulated data

In order to evaluate the performance of $\hat{\kappa}_y^2(f)$, discrete-time sequences $y[k]$ were simulated according to (13) with $x[k]$ being a train of unit impulses of frequency $f_e = 8$ Hz, $f_s = 2048$ Hz, $L = 4096$ points and $n[k]$, a zero mean, unit variance, white (Gaussian) noise. The value of $\kappa_y^2(f)$ was incremented from 0 to 1 in steps of 0.1 and its estimate calculated according to (3) with $M=12$ windows. The mean values of such estimates in the harmonics of f_e and in the other frequencies are displayed in Table 1. As it can be observed, the first converge to the theoretical values as $\kappa_y^2(f)$ becomes closer to one. On the other hand, the latter does not exhibit a trend with the increase of $\kappa_y^2(f)$. This result is theoretically expected, since the sampling distribution of $\hat{\kappa}_y^2(f)$ in such frequencies is independent of its true value $\kappa_y^2(f)$, and thus the probability of false alarm should be equal to the significance level α (in this case of 5%). Such result is also verified in Table 1 since the false positive rates shown vary randomly around 5%. The detection rate (obtained as the percentage of $\hat{\kappa}_y^2(f)$ - values in the harmonics of f_e which lie above its critical value) is also shown in Table 1, together with the theoretical probability of detection (PD) obtained according to (11). Good agreement between these values is observed.

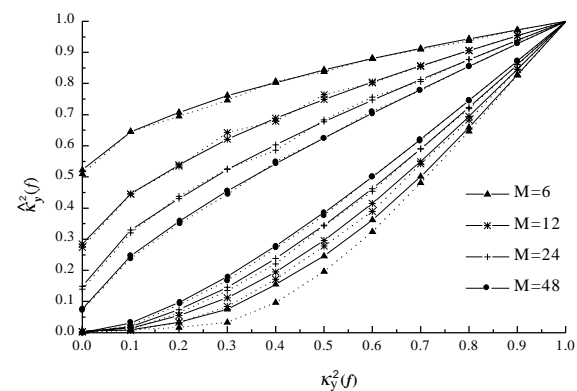


Figure 4. Confidence limits for $\hat{\kappa}_y^2(f)$ using Patnaik's approximation (solid lines) and obtained experimentally (dotted lines) for $M = 6, 12, 24$ and 48 .

Table 1. Performance of $\hat{\kappa}_y^2(f)$ with $M = 12$ for simulated signals.

	Mean in the harmonics	Mean outside the harmonics	False positive rate (%)	Detection rate (%)	SNR (dB)	PD (%)
$\kappa_y^2(f) = 0$	0.08	0.08	5.05	4.72	$-\infty$	5.00
$\kappa_y^2(f) = 0.1$	0.17	0.08	5.00	26.77	-9.54	25.70
$\kappa_y^2(f) = 0.2$	0.27	0.08	4.90	54.33	-6.02	52.29
$\kappa_y^2(f) = 0.3$	0.38	0.09	4.84	77.78	-3.68	77.82
$\kappa_y^2(f) = 0.4$	0.44	0.09	5.42	91.34	-1.76	92.61
$\kappa_y^2(f) = 0.5$	0.54	0.08	4.90	97.64	0.00	98.81
$\kappa_y^2(f) = 0.6$	0.61	0.09	5.81	100.00	1.76	99.95
$\kappa_y^2(f) = 0.7$	0.72	0.08	4.90	100.00	3.68	100.00
$\kappa_y^2(f) = 0.8$	0.82	0.08	4.74	100.00	6.02	100.00
$\kappa_y^2(f) = 0.9$	0.91	0.09	5.36	100.00	9.54	100.00
$\kappa_y^2(f) = 1.0$	1.00	0.08	4.74	100.00	$+\infty$	100.00

As it can be noted in Table 1, for $\hat{\kappa}_y^2(f)$ -values greater or equal to 0.6 the detection rate is virtually equal to one. However, the periodic component in signal $y[k]$ is not visually evident, as it is illustrated in Figure 5, where a stretch of 1 second is shown for $\hat{\kappa}_y^2(f) = 0.6$ (SNR = 1.76 dB). On the other hand, the plots of $\hat{\kappa}_y^2(f)$ as a function of frequency allow the identification of such periodic components, as it can be noted in Figure 6, where the peaks in the frequency $f_e = 8$ Hz and its harmonics become evident from $\hat{\kappa}_y^2(f) = 0.4$ (SNR = -1.76 dB).

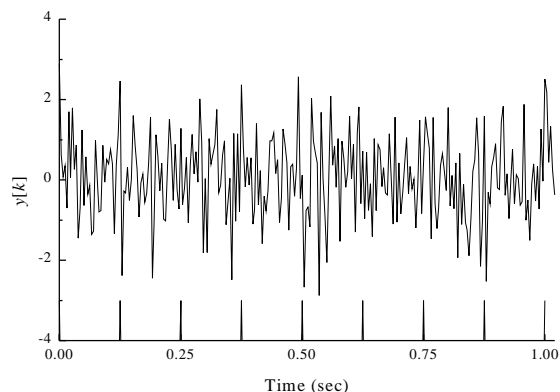


Figure 5. Signal $y[k]$ simulated using expression (13) for $\hat{\kappa}_y^2(f) = 0.6$. The unit impulse train mimicking the stimulation at 8 Hz is also shown.

Table 2 displays the theoretical (approximate) confidence limits for $\hat{\kappa}_y^2(f)$ with $M = 12$ calculated using (12), as well as the experimental ones that were obtained as the 2.5th and the 97.5th percentiles of the resultant distribution. As it can be noted, the range of variation of the estimates is compatible with the theoretically predicted one.

Application to EEG during photic stimulation

After the simulation study, we applied this analysis to the EEG signals from 14 normal young subjects (age range: 3 – 17 years) recorded over a period of 24 seconds during stroboscopic flash stimulation at 6 and 12 Hz. The signals from electrodes O1, O2, P3, P4, C3 and C4 (reference: ipsilateral earlobe) were recorded and digitised at 256 Hz. Next, stretches of signals were selected after about 1 second from the beginning of stimulation in order to ensure steady-state in the evoked responses. An inter-hemispheric analysis was carried out with $\hat{\kappa}_y^2(f)$ calculated using $M=12$ epochs and rectangular windows of 2 second duration.

Figure 7 shows a typical result (subject # 10 with intermittent $\hat{\kappa}_y^2(f)$ photic stimulation - IPS at 6 Hz) for all derivations, where $\hat{\kappa}_y^2(f)$ -values at homologue derivations exhibit similar values in the harmonics of the stimulation frequency. Such inter-hemispheric similarity was also verified for the other stimulation frequency, as it can be noted in Figure 8, which shows

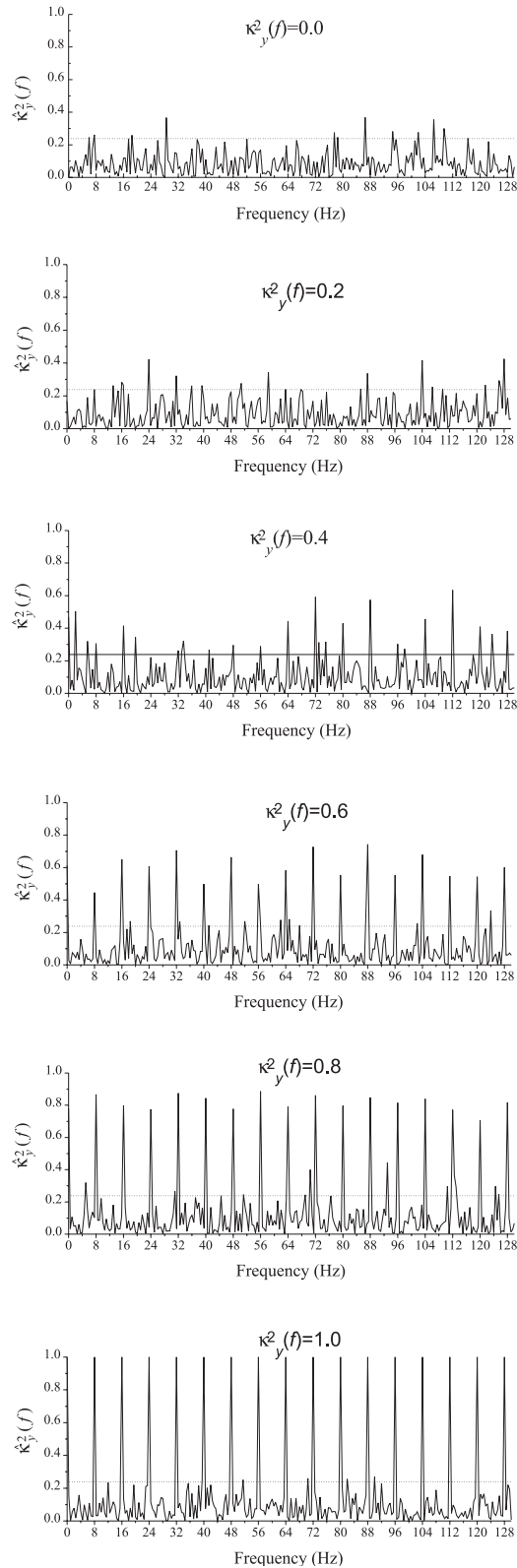


Figure 6. Plots of $\hat{\kappa}_y^2(f)$ for signals $y[k]$ generated according to (13) with theoretical values $\kappa_y^2(f)$ from 0 to 1 in steps of 0.2. Critical values are indicated in horizontal dotted lines.

Table 2. Confidence limits for $\hat{\kappa}_y^2(f)$ with $M = 12$.

	Theoretical Confidence limits (95%) of $\hat{\kappa}_y^2(f)$	Experimental Percentiles (2.5-97.5%) of $\hat{\kappa}_y^2(f)$
$\kappa_y^2(f) = 0$	0.00–0.29	0.00–0.27
$\kappa_y^2(f) = 0.1$	0.02–0.45	0.01–0.44
$\kappa_y^2(f) = 0.2$	0.05–0.54	0.05–0.53
$\kappa_y^2(f) = 0.3$	0.11–0.62	0.13–0.63
$\kappa_y^2(f) = 0.4$	0.19–0.69	0.19–0.68
$\kappa_y^2(f) = 0.5$	0.30–0.75	0.24–0.73
$\kappa_y^2(f) = 0.6$	0.42–0.80	0.37–0.79
$\kappa_y^2(f) = 0.7$	0.55–0.86	0.54–0.84
$\kappa_y^2(f) = 0.8$	0.69–0.91	0.71–0.91
$\kappa_y^2(f) = 0.9$	0.85–0.95	0.84–0.96
$\kappa_y^2(f) = 1.0$	1.00–1.00	1.00–1.00

$\hat{\kappa}_y^2(f)$ for the same subject with IPS at 12 Hz. It is interesting to note that the responses in this subject at the second harmonic when stimulating at 6 Hz are not always similar to that of the fundamental frequency when stimulating at 12 Hz. This becomes clear, for instance in derivations C3 and C4.

As one investigates the inter-hemispheric behaviour of $\hat{\kappa}_y^2(f)$ in the occipital regions (stronger responses to IPS), similar values are observed, as illustrated in Figure 9, which shows $\hat{\kappa}_y^2(f)$ (and its 95% confidence limits) at O1 and O2 for the 14 subjects in the first harmonic of stimulation frequency in 6 Hz. Considering the confidence limits, no statistically significant differences are observed between the inter-hemispheric values. It should be pointed out that in using the overlap of confidence limits obtained at $\alpha = 0.05$ to test differences, the resultant (bilateral) significance level is $2(\alpha/2)^2 = 0.00125$. Similar results (not shown) were observed for the first harmonic with IPS at 12 Hz.

In Figure 10, $\hat{\kappa}_y^2(f)$ is shown for electrode O1 in the first harmonic with stimulation at 12 Hz and in the second harmonic with stimulation at 6 Hz. Although the confidence limits of both estimates overlap in 10 subjects, $\hat{\kappa}_y^2(f)$ have very different values in four subjects (# 2, 6, 12 and 13). Thus the strength of the responses in 12 Hz for these four subjects varies if such frequency is the fundamental frequency of stimulation or the second harmonic of it.

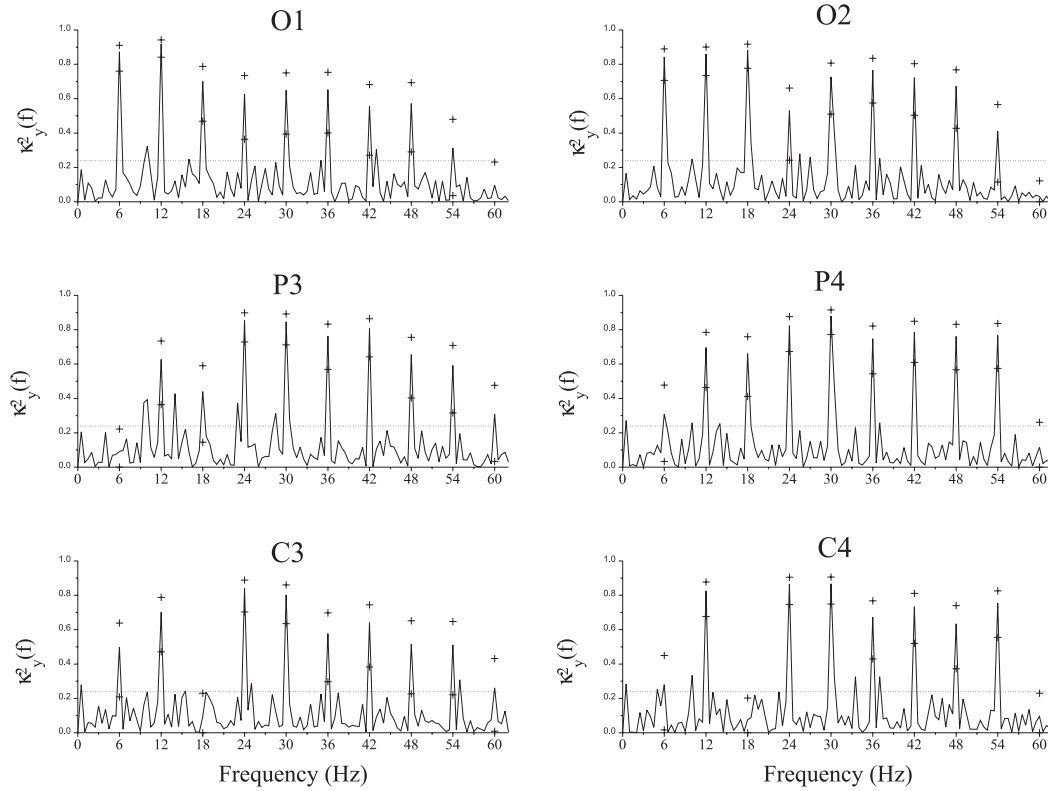


Figure 7. $\hat{K}_y^2(f)$ at derivations O1, O2, P3, P4, C3 and C4 of subject # 10 with IPS at 6 Hz. Critical values in dotted lines.

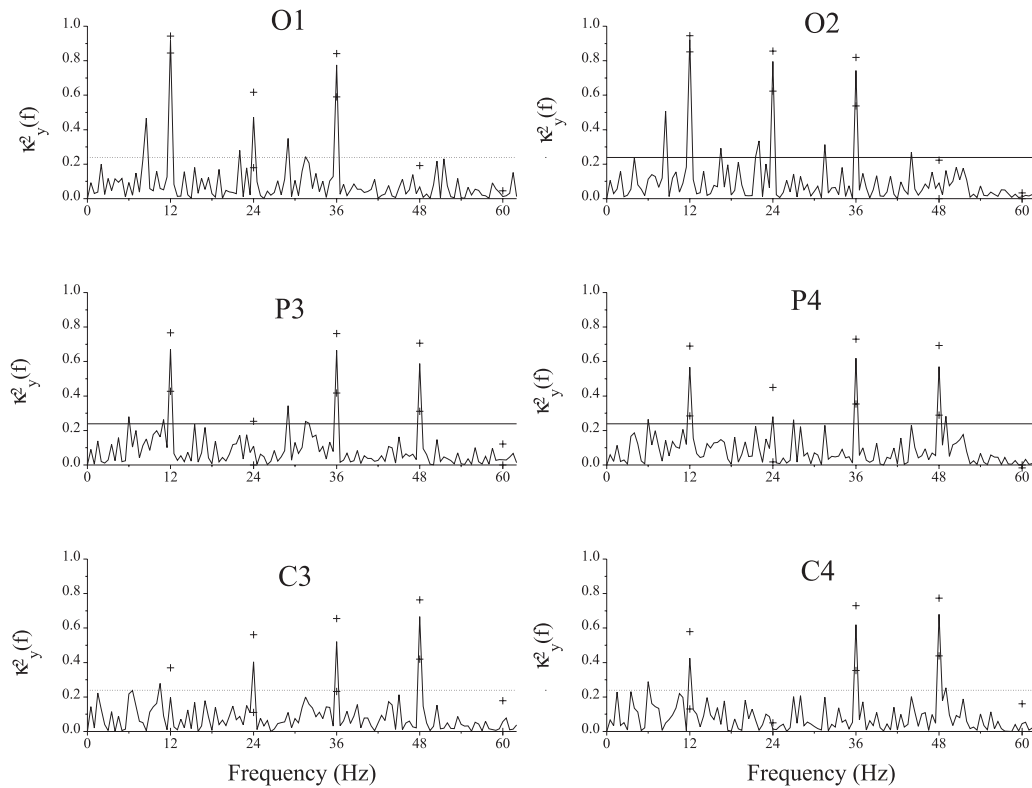


Figure 8. $\hat{K}_y^2(f)$ at derivations O1, O2, P3, P4, C3 and C4 of subject # 10 with IPS at 12 Hz. Critical values in dotted lines.

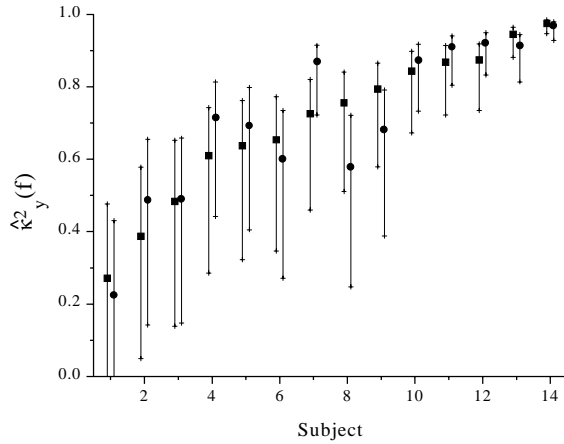


Figure 9. $\hat{\kappa}_y^2(f)$ at O1 (squares) and at O2 (circles) of the 14 subjects at the first harmonic of stimulation at 6 Hz. Confidence limits indicated as crosses.

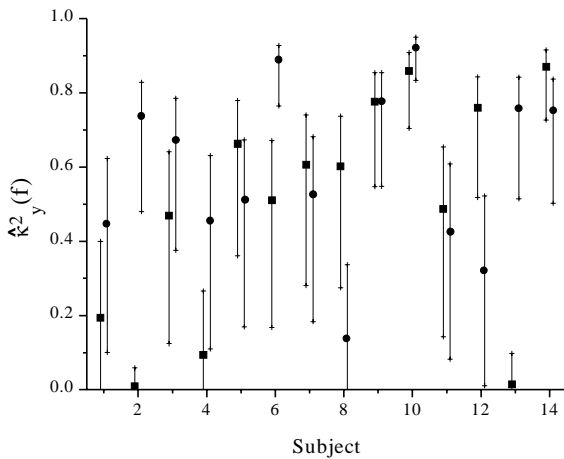


Figure 10. $\hat{\kappa}_y^2(f)$ at the first harmonic of stimulation at 12 Hz (circles) and at the second harmonic of stimulation at 6 Hz (squares) at O1 for the 14 subjects. Confidence limits indicated as crosses.

Conclusion

In this study, the sampling distribution for the coherence between one random and one periodic signal has been derived as in Miranda de Sá (2000) for the general case of nonzero coherence (hypothesis H_1). This allowed the probability of detecting an evoked response to be determined based on the coherence between EEG and stimuli. Our results show that in order to detect the responses in 95% of cases, a SNR of -7.9 dB is required with $M = 48$, SNR = -4.8 dB for $M = 24$, SNR = -1.2 dB for $M = 12$ and SNR = 2.5 dB for $M = 6$. In our case ($M = 12$) it would lead to a 95% probability of detection if an amplitude signal-to-noise ratio of 1:7 for visual responses with flash is assumed.

The confidence limits for these coherence estimates were also derived, using an approximation to the non-central F- distribution. This shows rather wide limits for low to mid-range coherences, which are rapidly reduced with increasing M . Monte Carlo simulation confirmed the validity of the theoretically derived limits.

The results from the application of the technique to EEG signals indicate an inter-hemispheric symmetry at homologue regions of many subjects in the stimulation frequency and also its harmonics. Such symmetry was more pronounced at occipital regions and is in agreement with Coull and Pedley (1978) who also stated that a reduced number of anomalies have been associated with asymmetric responses to photic stimulation. Thus an investigation of eventual $\hat{\kappa}_y^2(f)$ -asymmetries in signals from pathological subjects would be important in the evaluation of the diagnostic power of the technique. In addition, 28% of the subjects showed significant differences in the strength of the responses at 12 Hz depends on either such frequency was the stimulation frequency or the second harmonic of it. This difference may be due the fact that the stimulation frequency is lower or higher than the alpha rhythm of the subject, but this needs further investigation.

In conclusion, the present results extend the usefulness of coherence as a measure of stimulus responses, by providing a way of quantifying the degree of activation due to the stimulation. It allows inferring about the signal-to-noise ratio of the evoked responses as well as comparing responses at different cortical regions.

Appendix

The sampling distribution of $\hat{\kappa}_y^2(f)$ for the model of Figure 1 is now derived. Substituting $Y(f) = V(f) + N(f)$ in expression (3) we have:

$$\hat{\kappa}_y^2(f) = \frac{\left| \sum_{i=1}^M V(f) + N_i(f) \right|^2}{M \sum_{i=1}^M |V(f) + N_i(f)|^2} \quad (\text{A.1})$$

where M and N_i are defined as in (3) and $V(f)$ is the Fourier Transform of the evoked response $v[k]$, which will be assumed to be a real number (this does not reduce the generality of the proof, since data can always be rotated in such a way as to eliminate the imaginary part of $V(f)$, while for a stationary $n[k]$ the phase of $N(f)$ will keep uniformly distributed between

0 and 2π). The sum term in the denominator of (A.1) can be rewritten (f index omitted for simplicity) as:

$$\begin{aligned} \sum_{i=1}^M |V + N_i|^2 &= \sum_{i=1}^M [(V + N_i - V - \bar{N}) + V + \bar{N}]^2 \\ &= MV^2 + 2MV\bar{N}_R + M\bar{N}^2 + \sum_{i=1}^M |N_i - \bar{N}|^2 \end{aligned} \quad (\text{A.2})$$

where \bar{N}_R is the real part of mean value $\bar{N} = \frac{1}{M} \sum_{i=1}^M N_i$. Rewriting (A.1) using such result and expanding its numerator we have:

$$\hat{\kappa}_y^2 = \frac{M [MV^2 + 2MV\bar{N}_R + M\bar{N}^2]}{M [MV^2 + 2MV\bar{N}_R + M\bar{N}^2 + \sum_{i=1}^M |N_i - \bar{N}|^2]} \quad (\text{A.3})$$

which can be inverted to lead to the following relationship:

$$\frac{1}{\hat{\kappa}_y^2} = \frac{\sum_{i=1}^M |N_i - \bar{N}|^2}{[MV^2 + 2MV\bar{N}_R + M\bar{N}^2]} + 1 \quad (\text{A.4})$$

Further manipulations in (A.4) lead to:

$$\frac{\hat{\kappa}_y^2}{1 - \hat{\kappa}_y^2} = \frac{MV^2 + 2MV\bar{N}_R + M\bar{N}^2}{\sum_{i=1}^M |N_i - \bar{N}|^2} = \frac{M(V^2 + 2V\bar{N}_R + \bar{N}^2)}{\sum_{i=1}^M |N_i - \bar{N}|^2} \quad (\text{A.5})$$

Expressing \bar{N}^2 as a function of its both real and imaginary parts, expression (A.5) can be rewritten as:

$$\begin{aligned} \frac{\hat{\kappa}_y^2}{1 - \hat{\kappa}_y^2} &= \frac{M (V^2 + 2V\bar{N}_R + \bar{N}_R^2 + \bar{N}_I^2)}{\sum_{i=1}^M |N_i - \bar{N}|^2} \\ &= \frac{M [(V + \bar{N}_R)^2 + \bar{N}_I^2]}{\sum_{i=1}^M |N_i - \bar{N}|^2} = \frac{x_1^2 + x_2^2}{x_3} \end{aligned} \quad (\text{A.6})$$

where

$$x_1 = V + \bar{N}_R ; x_2 = \bar{N}_I ; x_3 = \frac{\sum_{i=1}^M |N_i - \bar{N}|^2}{M} \quad (\text{A.7})$$

The sampling distributions of the mean values \bar{N}_R and \bar{N}_I are easily obtained using the properties of Gaussian random variables, since N_R and N_I are zero mean, normally distributed, random variables with variance $\sigma_f^2 = \frac{L}{2} \sigma_n^2$ (Miranda de Sá, 2000, p. 140-141).

Thus it follows that:

$$\begin{cases} \bar{N}_R = \frac{1}{M} \sum_{i=1}^M N_{R_i} \\ \bar{N}_I = \frac{1}{M} \sum_{i=1}^M N_{I_i} \end{cases} \sim \frac{1}{M} \mathbf{N} \left(0, \frac{LM}{2} \sigma_n^2 \right) = \mathbf{N} \left(0, \frac{L}{2M} \sigma_n^2 \right) \quad (\text{A.8})$$

The distribution of the numerator of (A.6) – $(x_1^2 + x_2^2)$ – can be obtained based on the following relationship:

$$\left(\frac{x_1}{\sqrt{\frac{L}{2M} \sigma_n^2}} \right)^2 + \left(\frac{x_2}{\sqrt{\frac{L}{2M} \sigma_n^2}} \right)^2 \sim \chi_2'^2(\lambda) \quad (\text{A.9})$$

where $\chi_2'^2(\lambda)$ is the non-central chi-square distribution (Kay, 1998, p. 26) with two degrees of freedom and non-centrality parameter λ , which is given as the sum of the squared means of the unit variance Gaussian variables. In this case, since the mean of x_1 is equal to V and the mean of x_2 is equal to zero, λ is given as:

$$\lambda = \left(\frac{V}{\sqrt{\frac{L}{2M} \sigma_n^2}} \right)^2 + 0 = \frac{2MV^2}{L\sigma_n^2} \quad (\text{A.10})$$

Thus the distribution of the numerator of (A.6) is given as

$$x_1^2 + x_2^2 \sim \frac{L}{2M} \sigma_n^2 \chi_2'^2(\lambda) \quad (\text{A.11})$$

In order to derive the distribution of x_3 in (A.7), the following relationship may be used:

$$\sum_{i=1}^M |N_i - \bar{N}|^2 \sim \frac{L}{2} \sigma_n^2 \chi_{2(M-1)}^2 + \frac{L}{2} \sigma_n^2 \chi_{2(M-1)}^2 = \frac{L}{2} \sigma_n^2 \chi_{2(M-1)}^2 \quad (\text{A.12})$$

Since $\sum_{i=1}^M |N_i - \bar{N}|^2 = \sum_{i=1}^M (N_{R_i} - \bar{N}_R)^2 + \sum_{i=1}^M (N_{I_i} - \bar{N}_I)^2$ and, for independent Gaussian variables a_i , $\sum_{i=1}^M (a_i - \bar{a})^2 \sim \sigma_a^2 \chi_{2(M-1)}^2$ (Brownlee, 1965, cap. 8). Thus, dividing (A.12) by M we have:

$$x_3 \sim \frac{L}{2M} \sigma_n^2 \chi_{2(M-1)}^2 \quad (\text{A.13})$$

Using the results of (A.11) and (A.13), since x_1 , x_2 and x_3 are independent, it follows that:

$$\frac{\hat{\kappa}_y^2(f)}{1 - \hat{\kappa}_y^2(f)} = \frac{x_1^2 + x_2^2}{x_3} \sim \frac{\frac{L}{2M} \sigma_n^2 \chi_2^2(\lambda)}{\frac{L}{2M} \sigma_n^2 \chi_{2(M-1)}^2} \quad (A.14)$$

$$= F'_{2,2(M-1)}(\lambda) \cdot \frac{2}{2(M-1)}$$

where $F'_{2,2(M-1)}(\lambda)$ is the non-central F distribution (Kay, 1998, p. 29) with 2 and $2(M-1)$ degrees of freedom and non-centrality parameter $\lambda = \frac{2MV^2(f)}{L\sigma_n^2}$.

Thus, we finally have:

$$(M-1) \frac{\hat{\kappa}_y^2(f)}{1 - \hat{\kappa}_y^2(f)} \sim F'_{2,2(M-1)}(\lambda) \quad (A.15)$$

Acknowledgement

The authors acknowledge the assistance of Dr. V. Lazarev and the Laboratory of Clinical Neurophysiology of the Instituto Fernandes Figueira - FIOCRUZ, Rio de Janeiro, in data collection. This work received financial support of the CNPq and PRONEX / Ministry of Science and Technology, Brazil.

References

- Bendat, J.S., Piersol, G.G. (2000), *Random Data Analysis and Measurement Procedures*, third edition, New York: Wiley-Interscience.
- Brownlee, K.A. (1965), *Statistical Theory and Methodology in Science and Engineering*, New York: John Wiley & Sons, Inc.
- Carter, G.C. (1993), "Tutorial Overview of Coherence and Time Delay Estimation", In: *Coherence and Time Delay Estimation – An Applied Tutorial for Research, Development, Test, and Evaluation Engineers*, Ed.: G.C. Carter, New York: IEEE press, p. 1-27.
- Chiappa, K.H. (1997), *Evoked Potentials in Clinical Medicine*, second edition, New York: Raven Press.
- Coull, B.M. and Pedley, T.A. (1978), "Intermittent Photic Stimulation. Clinical Usefulness of non-Convulsive Responses", *Electroencephalography and Clinical Neurophysiology*, v. 44, n. 3, p. 353-363.
- Dobie, R. A. and Wilson, M. J. (1989): 'Analysis of auditory evoked potentials by magnitude-squared coherence', *Ear and Hearing*, v. 10, p. 2-13.
- Dobie, R. A. and Wilson, M. J. (1996): 'A comparison of t test, F test, and coherence methods of detecting steady-state Auditory-evoked potentials, distortion-product otoacoustic emissions, or other sinusoids', *J Acoust Soc Am*, v. 100, Pt. 12236-12246.
- Johnson, N.L., Kotz, S., Balakrishnan N. (1995), *Distributions in Statistics: Continuous Univariate Distributions* (Volume 2), New York: John Wiley & Sons, Inc.
- Kay, S. M. (1998): 'Fundamentals of Statistical Signal Processing volume II detection theory', New Jersey: Prentice-Hall.

Koopmans, L. H. (1974), *The spectral analysis of Time Series*, San Diego: Academic Press.

Miranda de Sá, A.M.F.L. (2000), *Desenvolvimento de Técnicas para o Estudo da Coerência no EEG durante Foto-Estimulação Intermitente*, Tese de Doutorado, Programa de Engenharia Biomédica, Rio de Janeiro, COPPE/UFRJ, 141 p., mar.

Miranda de Sá, A.M.F.L., Infantosi, A.F.C. and Simpson, D.M. (2001), "A statistical technique for measuring synchronism between cortical regions in the EEG during rhythmic stimulation", *IEEE Trans. Biomed. Eng.*, v. 40, n. 10, p. 1211-1215.

Miranda de Sá, A.M.F.L., Simpson, D.M., Infantosi, A.F.C. (2000), "Coherence between one random and one periodic signal – application to the EEG during sensory stimulation", *Digest of Papers of the 2000 World Congress on Medical Physics and Biomedical Engineering and the Proceedings of the 22nd Annual International Conference of the IEEE Engineering in Medicine and Biology Society*.

Nuttall, A. H. (1981): 'Invariance of distribution of coherence estimate to second-channel statistics', *IEEE Trans. Acoust. Speech, Signal Processing*, v. ASSP-29, p. 120-122.

Patnaik, P. B. (1949): 'The noncentral χ^2 and F-distributions and their applications', *Biometrika*, v. 36, p. 202-232.

Simpson, D. M., Tierra-Criollo, C. J., Leite, R. T., J.B. Zayen, J. B. and Infantosi, A. F. C. (2000): 'Objective response detection in an electroencephalogram during somatosensory stimulation', *Annals of Biomedical Engineering*, v. 28, p. 691-698.

